DESIGN AND OPTIMIZATION OF BULK MICROMACHINED ACCELEROMETER FOR SPACE APPLICATIONS

Thampi Paul[1] , Jaspreet Singh [2], M. M. Nayak [2],K. Rajanna [3] , M. Sasi Kumar [4]

[1]ISRO Inertial Systems Unit, Vattiyoorkavu, Thiruvananthapuram-695013, India.
[2]Semi-Conductor Laboratory (SCL), Dept. of Space, S A S Nagar-160071, India.
[3]Department of Instrumentation, Indian Institute of Science, Bangalore -560012, India.
[4]Dept. of Electronics & Communication, Marian Engg. College, Thiruvananthapuram -695082, India

thampi_paul@yahoo.co.uk, jaspreet@sclchd.co.in, mmnayak@gmail.com, kraj@isu.iisc.ernet.in

Abstract - The accelerometers used for Inertial Navigation in satellite launch vehicles demand excellent performance in terms of sensitivity, noise immunity, linearity, bias and scale factor stability over time and environmental changes. Detailed and in-depth design of the microstructure by computer simulation is required to ensure structural integrity and reliability of the microstructure. The microstructure of the accelerometer consists of a proof mass suspended from the mounting frame by beam springs. Extensive Finite Element simulation of the silicon microstructure has been carried out to obtain application specific optimum design parameters. Based on the deflection, frequency and stress analyses the optimum geometry and dimensions of the accelerometer have been determined. Noise analysis has been carried out, the performance of the accelerometer has been predicted and its compliance to the expected performance is ensured.

Index terms : Microstructure, Microelectromechanical Systems, Accelerometer

1. INTRODUCTION

The accelerometers used for Inertial Navigation in launch vehicles demand excellent performance in terms of sensitivity, noise immunity, linearity, bias and scale factor stability over time and environmental changes. Typical specifications of an accelerometer for launch vehicle applications are given in table 1. Reliable engineering design is called for to configure optimum geometry and dimensions of the microstructure of the accelerometer. Detailed and in-depth design of the microstructure by computer simulation is required to ensure structural integrity and reliability when it is subjected to specified loading at both normal operating and overload

conditions. In our present work, extensive Finite Element Simulation of silicon microstructure has been carried out to obtain specific design parameters and to predict the accelerometer performance. ANSYS as well as COVENTOR Finite Element tools have been used to design, model and characterize the mechanical microstructure. Noise analysis has been carried out for the designed accelerometer and the total noise figure has been computed including electronic circuit noise.

II. PRINCIPLE OF OPERATION

MEMS accelerometer consists of a proof mass which is suspended to a reference frame by spring elements as shown in figure 1. It consists of three bulk micromachined silicon parts (figure 1(a)) – Two silicon caps with shallow cavity for over-range/handling protection at bottom and top respectively and actual silicon micro-machined MEMS structure with proof mass suspended from a silicon frame via four beam springs at the middle. The bottom and top surfaces of the proof mass and shallow cavity surfaces of the silicon caps are metallised and electrical connections brought out. The three silicon parts are bonded together using silicon-to-silicon bonding technique. Acceleration causes displacement of the proof mass which is proportional to the acceleration. The displacement of the proof mass is determined by measuring the difference in capacitances between the proof mass and additional electrodes.

Table 1: Typical Specifications Of A Launch Vehicle Accelerometer

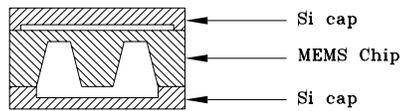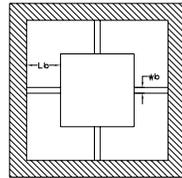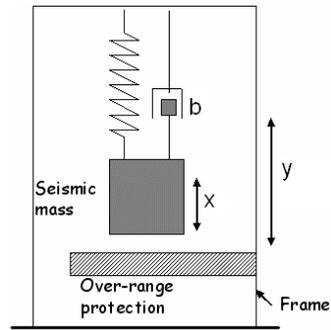| S.No.	Parameter	Value	Unit
1.	Range	±20	g
2.	Resolution	30	μg
3.	Output noise	2	μg/√Hz
4.	Linearity	<0.1	%
5.	Bias Stability	<300	μg
6.	Scale Factor Stability	<500	ppm
7.	Frequency Response	200	Hz
8.	Cross Axis Sensitivity	<1	%
9.	Temperature Range Operating Storage	 -10 to +70 -55 to +125	 Deg C Deg C
10.	Shock Survivability	1500	g

Figure 1(a & b): Basic Structure Of A Bulk-Micromachined Capacitive Accelerometer
Figure 2: Lumped Model Of A Capacitive Accelerometer

Figure 2 shows the lumped element model of such an accelerometer. When acceleration is applied, the displacement of the proof mass is detected as the change in capacitance between the fixed electrodes and movable proof-mass. Using D'Alembert's Principle, following equation of motion can be written from stationary observer point of view:

$$m\frac{\partial^2(x-y)}{\partial t^2} + b\frac{\partial x}{\partial t} + kx = 0$$

$$m\frac{\partial^2 x}{\partial t^2} + b\frac{\partial x}{\partial t} + kx = m\frac{\partial^2 y}{\partial t^2} \qquad \dots (1)$$

where

'y' is the movement of body of interest

'x' is the movement of the proof mass

'm' is the proof mass

'b' is the damping between the movable and fixed parts

'k' is the spring constant of the beam

With the help of Laplace Transform, its transfer function can be written as

$$\frac{X(s)}{A(s)} = \frac{1}{s^2 + s\dfrac{b}{m} + \dfrac{k}{m}} = \frac{1}{s^2 + s\dfrac{\omega_r}{Q} + \omega_r^2} \qquad \dots (2)$$

where

$$Q = \text{Quality Factor} = \frac{m\omega_r}{b}$$

A = Acceleration

ω_r = Resonance frequency = $\sqrt{\dfrac{k}{m}}$

At low frequency ($\omega \ll \omega_r$):

$$\frac{X}{A} = \frac{1}{\omega_r^2} \qquad \qquad \dots (3)$$

It is clear from the equation (3) that sensitivity is inversely proportional to the square of the resonant frequency. To obtain higher sensitivity with less noise, a large proof mass is needed which suggests the use of bulk micromachining technique. For optimal performance, hybrid solution has been chosen where sensor and electronics are realized on separate silicon chips but mounted in the same package. Here sensor and electronics can be optimized independently. Also the complexity of fabrication of sensor can be avoided. Z-axis accelerometers where sensitivity is normal to the proof mass plane are typically better than in-plane accelerometers.

III. DESIGN

Two components of the microstructure which dominantly characterize the accelerometer are proof mass and spring element. For better reproducibility and simplicity of fabricating, open loop architecture of the accelerometer is chosen. Also open loop architecture requires less die area compared to closed loop counterpart [2]. Open loop schemes tend to be relatively immune to small production variation in the transducer element and are inherently stable systems relying on no feedback signals. However the undesirable effects such as nonlinearity can be improved by software compensation [3].

Design objectives

The aim is to design a microstrucutre with the following objectives:

- Area of the silicon die to be minimum
- Area of the proof mass to be maximum/length of the beam to be minimum
- Maximum deflection to be ±0.6 microns for ± 20 g input
- Axial mode of frequency to be > 1000 Hz
- Cross axis sensitivity to be minimum
- Sufficient design margins with respect to operating loads.

Proof mass

Sensitivity of the capacitive sensing accelerometer is directly proportional to the area of the parallel plates (area of the proof mass). The design constraint is that the silicon die area has to be minimum. A trade off has to be made between the proof mass area and sensitivity. A square geometry is selected for the proof mass to keep the effects of thermal expansion to a minimum so that accelerometers do not require any active temperature compensation. From the manufacturing point of view, a typical 3 mm square proof mass with 250-micron thickness has been chosen.

Beam springs

A multiple beam symmetrical suspension structure employing four beam springs as shown in fig.1(b) is chosen. Here the acceleration in the sensitive axis causes a translational motion of the proof mass while acceleration in other two axes causes rotation of the proof mass reducing cross axis sensitivity.

The nomenclatures used in this analysis are as follows:

The beam thickness is denoted as T_b

The beam width is denoted as W_b

The beam length is denoted as L_b

IV. ANAYLYSIS

MESH CONVERGENCE

ANSYS shell element SHELL63 is taken for the Finite Element (FE) modeling of the microstructure. SHELL63 has both bending and membrane capabilities. Both in-plane and normal load are permitted. The element has six degrees of freedom at each node: translations in the nodal x, y and z directions and rotations about the nodal x, y and z-axes. Stress stiffening and large deflection capabilities are included. Typical dimensions of the beam and proof mass are assumed. Maximum deflection for the same input and same location is studied to arrive at the optimum number of elements. The results of the mesh convergence study are given in table 2. The results are more or less converging at Sl.No.3 of table 2, hence the total number of elements taken for all analyses is 7541.

Table 2: Results Of Mesh Convergence Study

Sl No.	No. of nodes	No. of elements	Deflection (μm)
1	3638	3475	0.5371
2	5390	5191	0.5491
3	7776	7541	0.5503
4	10203	9932	0.5506

STRUCTURAL OPTIMIZATION ON THE BEAM SPRINGS

Initial gap: For capacitance transduction circuit, sensitivity is inversely proportional to the square of initial gap between movable and fixed capacitor plates. It is better to select a gap as small as possible considering the bulk micromachining capability. An initial gap of 2 micron is easily feasible for fabrication.

Deflection: Having fixed initial gap for the capacitive sensing as 2um, due to stiction the maximum full-scale deflection allowed is limited to 30% of the initial gap i.e.0.6μm [4]. To achieve maximum sensitivity (1.31 pF/g) beam spring dimensions are designed in such a way that the proof mass is deflected ±0.6 micron for full scale input of ±20g. The non-linearity of delta C versus deflection corresponding to 0.6μm has been computed as 2.83%. This figure can be improved by software compensation. Using the third order polynomial, the linearity improves to 0.036% [3].

To start with, initial dimensions of the beam springs (fig.1) are taken as Lb = 300 micron, Wb = 150 μm & Tb = 10 μm.

DEFLECTION ANALYSIS

Parametric analysis is performed to fix the beam dimensions so as to achieve deflection around 0.6 micron for full scale input of 20g. The deflection of the proof mass for 20 g input is studied by varying beam length for different values of beam thickness keeping beam width constant and also for different values of beam width keeping beam thickness constant. The plots are given in figure-3 and 4 respectively.

Feasible options: A set of beam dimensions resulting in around 0.6 micron deflection for 20g input was selected as feasible options in the first iteration. Thus the feasible options are given in table-3. Considering the beam length alone, sl.no. 4 having least beam length is the best option.

Table 3: Feasible Options After Deflection Analysis

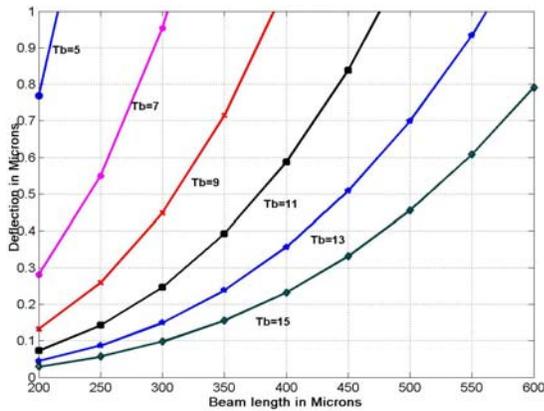| Sl. No	Beam Thickness Tb (µm)	Beam width Wb (µm)	Beam length Lb (µm)	Deflection (µm)
1	7	150	250	0.55
2	9	150	333	0.60
3	11	150	415	0.60
4	7	100	225	0.60
5	7	200	282	0.60

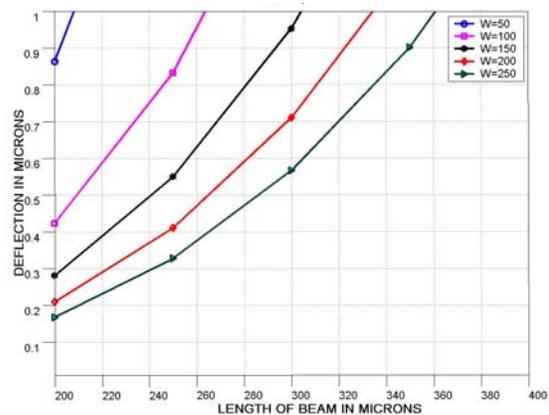Figure 3: Deflection Versus Beam Length For 20g Input; W_b=150 µm And Varying T_b (Axial Mode)

Figure 4: Deflection Versus Beam Length For 20g Input; T_b=7 µm And Varying W_b (Axial Mode)

FREQUENCY ANALYSIS

The microstructure will have three basic modes of vibration (x, y, z) with fundamental resonant frequency determined mainly by the dimensions of the beam. Engineering design of the microstructure is to avoid resonant vibration by raising the natural frequency of the structure so that all conceivable frequencies of all modes of induced vibration by the applied excitation force will not reach even the lowest of all modes of natural frequency. To study the natural frequency of the structure, a normal mode analysis is performed on all feasible options in table 3 by varying the beam length for different values of beam thickness keeping beam width constant and as well as different values of beam width keeping the beam thickness constant. The natural frequency versus beam length in first mode is plotted in figure 5 and 6 respectively.

From the dynamic analysis, it is observed that though the beam length in sl.no. 4 is the

lowest, its natural frequency is over 4000Hz, whereas sl.no. 1 is having a natural frequency of 3003Hz. A trade off has to be made between beam length and natural frequency. For better sensitivity, natural frequency has to be smaller and hence sl.no. 1(table-3) is the preferred option from now on.
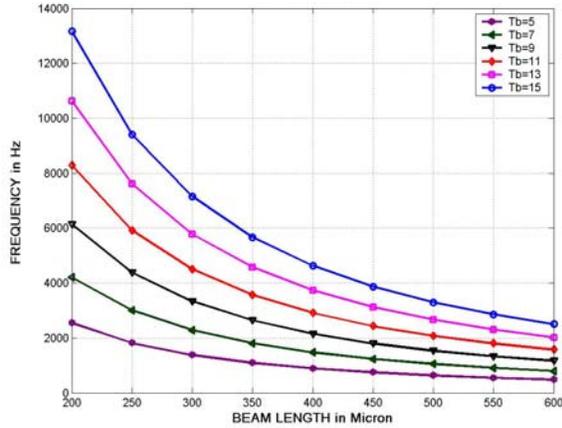

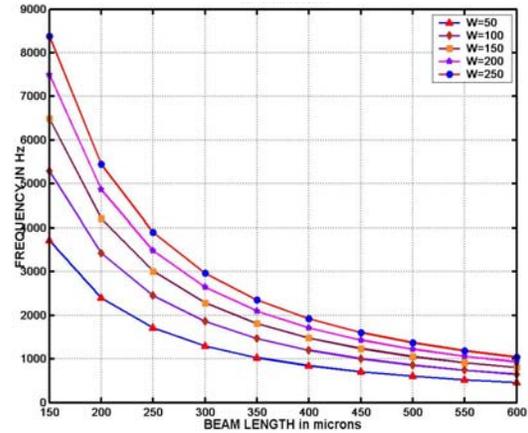Figure 5: Natural Frequency Versus Beam Length. For Wb=150 μm And Varying T_b (Axial Mode)

Figure 6: Natural Frequency Versus Beam Length. For T_b=7 μm And Varying W_b (Axial Mode)

STRESS ANALYSIS

A quasi static load of 20g is applied along the sensing axis to find the maximum von-mises stress for all the options in table 3.Stress versus length plots for varying Tb keeping W_b constant and for varying W_b keeping T_b constant are given in figure 7&8 respectively. From the stress analysis it is found that sl.no.1 in table 3 has sufficiently high factor of safety (FS) of 230. Based on the analysis, sl.no 1 is the best among all options studied till now and is designated as option-1. The analysis results of optimized microstructure (option-1) are given in table 4.

Table 4: Analysis Results Of Option – 1

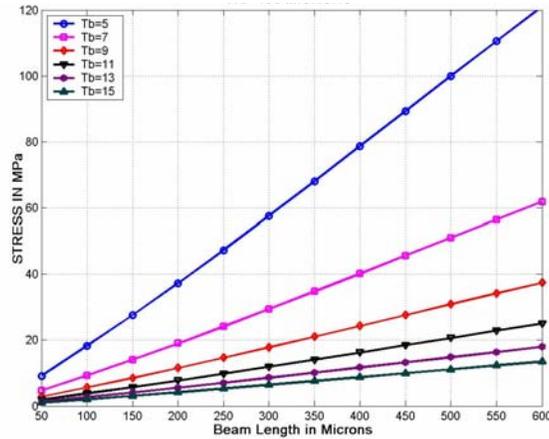| L_b (μm)	W_b (μm)	T_b (μm)	Deflection (μm)	Frequency (Hz)	FS
250	150	7	0.55	3003	230

Figure 7: Stress Versus Beam Length For W_b=150 µm And Varying T_b (Axial Mode)
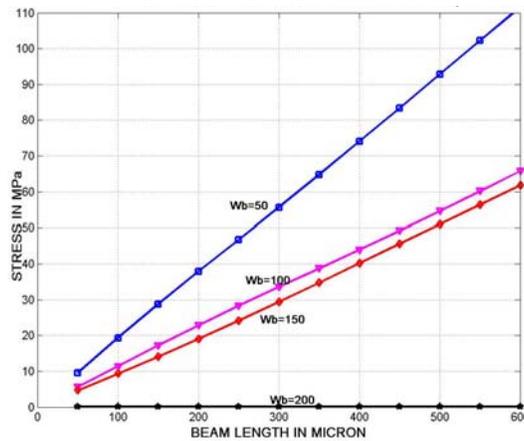

Figure 8: Stress versus Beam Length For T_b=7 µm And Varying W_b (Axial Mode)

GEOMETRY OPTIMIZATION
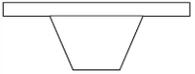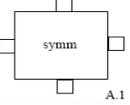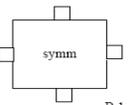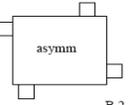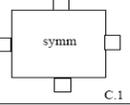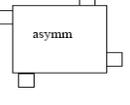
In the structural analysis, one typical symmetrical suspension structure (Fig.1) was chosen. For optimizing the geometry of the microstructure, several other suspension structures that can be used in bulk micromachined accelerometers given in table 5 were also analyzed. The beams were assumed to be rigidly fixed. The same number of elements was assumed in all cases. The first two modes of frequency are taken for comparative study. Table 5 gives the comparison of sensitivity, cross-axis sensitivity and modal frequencies for various structures.

It is observed that there is no significant difference in the Wet Etching options A.1 and A.2 as far as the defection for 20 g and first mode of natural frequency is concerned. But when the Dry Etching options (B & C) are explored, it is found that option-C.2 is giving the least cross-axis sensitivity with considerable margin in resonance frequency. Also from process point of view this

structure is simple to fabricate.

Table 5: Analysis Results Of Geometry Optimization Study

Cross-section	Top view	Deflection (δ) μm		Modal Frequencies (kHz)
		$a = a_z = 20g$ (sensing axis)	$a = a_x = 20g$ (lateral axis)	
A	A.1 symm	$\delta_z = 0.512$	$\delta_z = 0.067$	3.120, 4.663
	A.2 asymm	$\delta_z = 0.512$	$\delta_z = 0.051$	3.120, 4.955
B	B.1 symm	$\delta_z = 0.564$	$\delta_z = 0.077$	2.972, 3.890
	B.2 asymm	$\delta_z = 0.566$	$\delta_z = 0.051$	2.964, 4.793
C	C.1 symm	$\delta_z = 0.465$	$\delta_z = 5.2e\text{-}6$	3.277, 4.333
	C.2 asymm	$\delta_z = 0.555$	$\delta_z = 6.7e\text{-}6$	2.995, 4.891
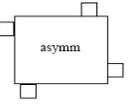
NOISE ANALYSIS

Mechanical Noise: The performance of accelerometers is limited by the thermal motion of the proof mass. Lesser proof mass of the micromachined accelerometers results in rather large movements. An equivalent acceleration spectral density, the so-called Total Noise Equivalent Acceleration (TNEA) is given by [1]

$$TNEA = \sqrt{\frac{4 k_B T \omega_r}{Qm}}$$

where k_B is Boltzman constant,

T   is temperature in Kelvin

ω_r is resonant frequency of the microstructure

m   is mass of the proof mass

Q   is quality factor

By packaging at reduced pressure, damping factor can be tuned to a value as low as 2e-3 corresponding to Q factor of 50.

Assuming Q value of 50, TNEA = 1.1 μg/√Hz

Electronic Circuit Noise: Electronic circuit noise can also limit the overall noise figure. By selecting special low noise devices for the capacitance readout circuit, it is possible to reduce the circuit noise to as low as 0.04μg /√Hz. [5]

Resolution: Resolution is limited by the overall noise figure. The estimated overall noise figure is 1.14 μg /√Hz. Noise equivalent acceleration for 200 Hz bandwidth is 16.07 μg.

V. RESULTS

The designed and optimized dimensions (C.2) of the application specific ±20g, 200 Hz MEMS accelerometer for launch vehicle applications are given below:

Proof-mass area (A)	:	3000x3000 μm^2
Proof-mass thickness (Tm)	:	250 μm
Beam length (Lb)	:	250 μm
Beam width (Wb)	:	150 μm
Beam Thickness (Tb)	:	7 μm

Predicted performance of the designed accelerometer:

Range	:	±20g
Bandwidth	:	200 Hz
Linearity	:	0.036 %(after software compensation)
Modal frequency		
Axial	:	2995 Hz
Modes2&3	:	4891Hz
Factor of safety	:	230
Sensitivity	:	1.31 pF/g
Noise	:	1.14 μg /√Hz.
Resolution	:	better than 20 ug

VI. CONCLUSION

Microstructure of an application specific MEMS accelerometer for ± 20g, 200 Hz for launch vehicle applications has been designed, optimized and its performance predicted.

REFERENCES

[1] Elwenspoek, "Mechanical Microsensors," Springer, 2001

[2] Gad-El-Hak & Mohamed, "MEMS Hand Book,"CRC Press, Boca raton, 2002.

[3] Thampi Paul P, Vijin Jenius S and Sasikumar M, "Characterization and Nonlinearity compensation of Capacitive sensing MEMS accelerometer for launch vehcle applications," in Proceedings of the National Society for Insturmentation of ISOI (NSI-30), 2005, pp. 417-421.

[4] Hsu & Tai-Ran, "MEMS and Microsystems-Design and Manufacture," Tata McGraw-Hill, New Delhi, 2002

[5] Thampi Paul, Roy Paul V and Sasikumar M, "Design and Analysis of High performance differential capacitance readout circuit for Navigational grade MEMS accelerometer," in Proceedings of the National Society for Instrumentation of ISOI (NSI-30), 2005, pp. 410-416.

[6] Fraden, "Hand Book of Modern Sensors-Physics, Design and Application," Springer, New York 2004